

# Exclusive Double Diffractive Higgs Boson Production at LHC.

Petrov V.A. and Ryutin R.A.  
Institute for High Energy Physics  
*142 281* Protvino, Russia

## Abstract

Exclusive double diffractive (EDD) Higgs boson production is analyzed in the framework of the Regge-eikonal approach. Total and differential cross-sections for the process  $p + p \rightarrow p + H + p$  are calculated. Experimental possibilities to find Higgs boson at LHC are discussed.

## Keywords

Diffractive Higgs Boson Production – Pomeron – Regge-Eikonal model

# 1 Introduction

LHC collaborations aimed at working in low (TOTEM)- and high (CMS)- $p_T$  regimes related to typical undulatory (diffractive) and corpuscular (point-like) behaviours of the corresponding cross-sections may offer a very exciting possibility to observe an interplay of both regimes [1]. In theory the "hard part" can be (hopefully) treated with perturbative methods whilst the "soft" one is definitely nonperturbative.

Below we give an example of such an interplay: exclusive Higgs boson production by diffractively scattered protons, i.e. the process  $p + p \rightarrow p + H + p$ , where  $+$  means also a rapidity gap.

This process is related to the dominant amplitude of exclusive two-gluon production. Driving mechanism of the diffractive processes is the Pomeron. Data on the total cross-sections demands unambiguously for the Pomeron with larger-than-one intercept, thereof the need in "unitarisation".

As will be seen below the detection of the Higgs boson (in the  $b\bar{b}$  mode) at LHC in the double diffractive regime looks fairly possible.

## 2 Calculations

In Figs. 1,2 we illustrate in detail the process  $p + p \rightarrow p + H + p$ . Off-shell proton-gluon amplitudes in Fig. 2 are treated by the method developed in Ref. [2], which is based on the extension of Regge-eikonal approach, and succesfully used for the description of the HERA data [3].

The amplitude of the process  $p + p \rightarrow p + H + p$  consists of two parts (see Fig. 2). The "hard" part  $F$  is the usual gluon-gluon fusion process calculated in the Standard Model[4]. "Soft" amplitudes  $T_{1,2}$  are obtained in the Regge-eikonal approach.

We use the following kinematics, which corresponds to the double Regge limit. It is convenient to use light-cone components  $(+, -, \perp)$ . The components of momenta of the hadrons in Fig. 2 are

$$\begin{aligned}
 p_1 &= \left( \sqrt{\frac{s}{2}}, \frac{m^2}{\sqrt{2s}}, \mathbf{0} \right) \\
 p_2 &= \left( \frac{m^2}{\sqrt{2s}}, \sqrt{\frac{s}{2}}, \mathbf{0} \right) \\
 p'_1 &= \left( (1 - \xi_1) \sqrt{\frac{s}{2}}, \frac{\Delta_1^2 + m^2}{(1 - \xi_1) \sqrt{2s}}, -\Delta_1 \right) \\
 p'_2 &= \left( \frac{\Delta_2^2 + m^2}{(1 - \xi_2) \sqrt{2s}}, (1 - \xi_2) \sqrt{\frac{s}{2}}, -\Delta_2 \right) \\
 q &= (q_+, q_-, \mathbf{q}) , \\
 q_1 &= q + p_1 - p'_1 = q + \Delta_1 , \\
 q_2 &= -q + p_2 - p'_2 = -q + \Delta_2 ,
 \end{aligned} \tag{1}$$

$\xi_{1,2}$  are fractions of protons momenta carried by gluons. For two-dimensional transverse

vectors we use boldface type. From the above notations we can obtain the relations:

$$\begin{aligned}
t_{1,2} &= \Delta_{1,2}^2 \simeq -\frac{\Delta_{1,2}^2(1 + \xi_{1,2}) + \xi_{1,2}^2 m^2}{1 - \xi_{1,2}} \simeq -\Delta_{1,2}^2, \quad \xi_{1,2} \rightarrow 0 \\
\cos \phi_0 &= \frac{\Delta_1 \Delta_2}{|\Delta_1| |\Delta_2|} \\
M_H^2 &\simeq \xi_1 \xi_2 s + t_1 + t_2 - 2\sqrt{t_1 t_2} \cos \phi_0 \\
(p_1 + q)^2 &\simeq m^2 + q^2 + \sqrt{2s} q_- = s_1 \\
(p_2 - q)^2 &\simeq m^2 + q^2 - \sqrt{2s} q_+ = s_2.
\end{aligned} \tag{2}$$

Physical region of diffractive events with two rapidity gaps is defined by the following kinematical cuts:

$$0.01 \text{ GeV}^2 \leq |t_{1,2}| \leq 1 \text{ GeV}^2, \tag{3}$$

$$\xi_{min} \simeq \frac{M_H^2}{s \xi_{max}} \leq \xi_{1,2} \leq \xi_{max} = 0.1, \tag{4}$$

$$\begin{aligned}
(\sqrt{-t_1} - \sqrt{-t_2})^2 &\leq \kappa \leq (\sqrt{-t_1} + \sqrt{-t_2})^2 \\
\kappa &= \xi_1 \xi_2 s - M_H^2 \ll M_H^2
\end{aligned} \tag{5}$$

We can write the relations in terms of  $y_{1,2}$  and  $y_H$  (hadron and Higgs boson rapidities correspondingly):

$$\begin{aligned}
\xi_{1,2} &\simeq \frac{M_H}{\sqrt{s}} e^{\pm y_H}, \\
|y_H| &\leq y_0 = \ln \left( \frac{\sqrt{s} \xi_{max}}{M_H} \right), \\
y_0 &\simeq 2.5 \quad \text{for} \quad \sqrt{s} = 14 \text{ TeV}, \quad M_H = 115 \text{ GeV}, \\
|y_{1,2}| &= \frac{1}{2} \ln \frac{(1 - \xi_{1,2})^2 s}{m^2 - t_{1,2}} \geq 9
\end{aligned} \tag{6}$$

The calculation of the amplitude is based on the nonfactorized scheme. The contribution of the diagram depicted in Fig. 2 is obtained by integrating over all internal loop momenta. It was shown in [5], that the leading contribution arises from the region of the integration, where momentum  $q$  is "Glauber-like", i.e. of the order  $(\mathbf{k}_+ m^2 / \sqrt{s}, \mathbf{k}_- m^2 / \sqrt{s}, \mathbf{k} m)$ , where  $\mathbf{k}$ 's are of the order 1. The detailed consideration of the loop integral like

$$\int \frac{d^4 q}{(2\pi)^4} \frac{f(q, p_1, p_2, \Delta_1, \Delta_2)}{(q^2 + i0)(q_1^2 + i0)(q_2^2 + i0)} \tag{7}$$

shows that the main contribution comes from the poles

$$\begin{aligned}
q_1^2 &= \sqrt{2s} \xi_1 q_- - \mathbf{q}_1^2 = 0, \\
q_2^2 &= -\sqrt{2s} \xi_2 q_+ - \mathbf{q}_2^2 = 0.
\end{aligned}$$

In this case

$$q = \left( -\frac{\mathbf{q}_2^2}{\xi_2 \sqrt{2s}}, \frac{\mathbf{q}_1^2}{\xi_1 \sqrt{2s}}, \mathbf{q} \right), \quad (8)$$

where

$$\begin{aligned} \mathbf{q}_1^2 &= \mathbf{q}^2 + \Delta_1^2 + 2|\mathbf{q}||\Delta_1| \cos(\phi + \frac{\phi_0}{2}), \\ \mathbf{q}_2^2 &= \mathbf{q}^2 + \Delta_2^2 - 2|\mathbf{q}||\Delta_2| \cos(\phi - \frac{\phi_0}{2}) \end{aligned}$$

In this region  $|q^2/M_H^2| \ll 1$ , and for the  $ggH$ -vertex  $F^{\mu\nu}$  in the first order of the strong coupling we have the usual [4] expression

$$F^{\mu\nu} \simeq \left( g^{\mu\nu} - \frac{2q_2^\mu q_1^\nu}{M_H^2} \right) F_{gg \rightarrow H}, \quad (9)$$

$$F_{gg \rightarrow H} = M_H^2 \frac{\alpha_s}{2\pi} \sqrt{\frac{G_F}{\sqrt{2}}} f(\eta), \quad (10)$$

$$f(\eta) = \frac{1}{\eta} \left\{ 1 + \frac{1}{2} \left( 1 - \frac{1}{\eta} \right) \left[ Li_2 \left( \frac{2}{1 - \sqrt{1 - \frac{1}{\eta}} - i0} \right) + Li_2 \left( \frac{2}{1 + \sqrt{1 - \frac{1}{\eta}} + i0} \right) \right] \right\},$$

where  $\eta = M_H^2/4m_t^2$ ,  $G_F$  is the Fermi constant. NLO K-factor 1.5 for the  $gg \rightarrow H$  process is included to the final answer.

Taking the general form for  $T$ -amplitudes that satisfy identities

$$q^\alpha T_{\mu\alpha}^D = 0, \quad q_i^\mu T_{\mu\alpha}^D = 0, \quad (11)$$

and neglecting terms of the order  $o(\xi_i)$ , the following expression is found at  $|t_i| \leq 1 \text{ GeV}^2$ :

$$T_{\mu\alpha}^D(p, q, q_i) = \left( G_{\mu\alpha} - \frac{P_\mu^{q_i} P_\alpha^q}{P_{q_i} P_q} \right) T_{gp \rightarrow gp}^D(s_i, t_i, qq_i) \quad (12)$$

$$G_{\mu\alpha} = g_{\mu\nu} - \frac{q_{i,\mu} q_{\alpha}}{qq_i},$$

$$P_\mu^{q_i} = p_\mu - \frac{pq_i}{qq_i} q_\mu,$$

$$P_\alpha^q = p_\alpha - \frac{pq}{qq_i} q_{i,\alpha}.$$

For  $T_{gp \rightarrow gp}^D$  we use the Regge-eikonal approach [2, 6]. At small  $t_i$  it takes the form of the Born approximation, i.e. Regge factor:

$$T_{gp \rightarrow gp}^D(s_i, t_i, qq_i) = c_{gp} \left( e^{-i\frac{\pi}{2} \frac{s_i - qq_i - m^2}{s_0 - qq_i - m^2}} \right)^{\alpha_P(t_i)} e^{b_0 t_i}, \quad (13)$$

$$b_0 = \frac{1}{4} \left( \frac{r_{pp}^2}{2} + r_{gp}^2 \right),$$

where  $\alpha_P(0) = 1.203$ ,  $\alpha'_P(0) = 0.094 \text{ GeV}^{-2}$ ,  $r_{pp}^2 = 2.477 \text{ GeV}^{-2}$  are found in [6]. Parameters  $c_{gp} \simeq 3.5$ ,  $r_{gp}^2 = 2.54 \text{ GeV}^{-2}$  are defined from fitting the HERA data on elastic  $J/\Psi$  production, which will be published elsewhere. The upper bound for the constant  $c_{gp}^{up} \simeq 2.3(3.3)$  can be also estimated from the exclusive double diffractive di-jet production at Tevatron, if we take CDF cuts and the upper limit for the exclusive total di-jet cross-section [7]. The effective value  $c_{gp} = 2.3$  corresponds to the case, when the Sudakov suppression factor is absorbed into the constant, and  $c_{gp} = 3.3$  is obtained when taking into account this factor explicitly.

The full amplitude for Higgs boson production looks as follows:

$$T_{pp \rightarrow pHp} \simeq \int \frac{d^4 q}{(2\pi)^4} \frac{8F^{\mu\nu}(q_1, q_2) T_{\mu\alpha}^D(p_1, q, q_1) T_{\nu\alpha}^D(p_2, -q, q_2)}{(q^2 + i0)(q_1^2 + i0)(q_2^2 + i0)}. \quad (14)$$

Factor 8 arises from the colour index contraction. Let  $l^2 = -q^2 \simeq \mathbf{q}^2$ ,  $y_H = \langle y_H \rangle = 0$  and contract all the tensor indices, then the integral (14) takes the form

$$T_{pp \rightarrow pHp} \simeq c_{gp}^2 e^{b(t_1+t_2)} \frac{\pi}{(2\pi)^2} \left( -\frac{s}{M_H^2} \right)^{\alpha_P(0)} \cdot 8F_{gg \rightarrow H} \cdot I, \quad (15)$$

$$b = \alpha'_P(0) \ln \left( \frac{\sqrt{s}}{M_H} \right) + b_0, \quad (16)$$

$$I \simeq \int_0^{M_H^2} \frac{dl^2}{l^4} \left( \frac{l^2}{s_0 - m^2 + l^2/2} \right)^{2\alpha_P(0)} \simeq 1.88 \text{ GeV}^{-2}, \quad (17)$$

where  $M_H = 100 \text{ GeV}$ , and  $s_0 - m^2 \simeq 1 \text{ GeV}^2$  is the scale parameter of the model that is used in the global fitting of the data on  $pp(p\bar{p})$  scattering for on-shell amplitudes [6]. It remains fixed in the present calculations.

If we take into account the emission of virtual "soft" gluons, while prohibiting the real ones, that could fill rapidity gaps, it results in the Sudakov-like suppression [8]:

$$F_s(l^2) = \exp \left[ -\frac{3}{2\pi} \int_{l^2}^{M_H^2/4} \frac{dp_T^2}{p_T^2} \alpha_s(p_T^2) \ln \left( \frac{M_H^2}{4p_T^2} \right) \right], \quad (18)$$

and to the new value of the integral (17):

$$I_s \simeq \int_0^{M_H^2} \frac{dl^2}{l^4} F_s(l^2) \left( \frac{l^2}{s_0 - m^2 + l^2/2} \right)^{2\alpha_P(0)} \simeq 0.38 \text{ GeV}^{-2}, M_H = 100 \text{ GeV}. \quad (19)$$

In this case the total cross-section becomes 24 times smaller, than without the factor  $F_s$ .

Unitarity corrections can be estimated from the elastic  $pp$  scattering by the method depicted in Fig.1, where

$$T_X = T_{pp \rightarrow pHp}, \quad (20)$$

$$\begin{aligned}
V(s, \mathbf{q}_T) &= 4s(2\pi)^2 \delta^2(\mathbf{q}_T) + 4s \int d^2\mathbf{b} e^{i\mathbf{q}_T \mathbf{b}} \left[ e^{i\delta_{pp \rightarrow pp}} - 1 \right], \\
T_X^{Unit.}(p_1, p_2, \Delta_1, \Delta_2) &= \frac{1}{16ss'} \int \frac{d^2\mathbf{q}_T}{(2\pi)^2} \frac{d^2\mathbf{q}'_T}{(2\pi)^2} V(s, \mathbf{q}_T) \cdot T_X(p_1 - q_T, p_2 + q_T, \Delta_{1T}, \Delta_{2T}) \cdot \\
&\quad \cdot V(s', \mathbf{q}'_T), \\
\Delta_{1T} &= \Delta_1 - q_T - q'_T, \\
\Delta_{2T} &= \Delta_2 + q_T + q'_T,
\end{aligned}$$

and  $\delta_{pp \rightarrow pp}$  can be found in Ref. [6]. It reduces the integrated cross-section by the factor about 14.

### 3 Results and discussions

We have the following expression for the differential cross-section:

$$\begin{aligned}
\frac{d\sigma}{dt_1 dt_2 d\xi_1 d\xi_2} &= \frac{\pi |T_{pp \rightarrow pHp}^{Unit.}|^2}{8s(2\pi)^5 \sqrt{-\lambda}} \\
\lambda &= \kappa^2 + 2(t_1 + t_2)\kappa + (t_1 - t_2)^2 \leq 0
\end{aligned} \tag{21}$$

By partial integrating (21) we obtain the cross-sections  $d\sigma/dt$  and  $d\sigma/d\xi$ . The first result of our calculations is depicted in the Fig. 3. The antishrinkage of the diffraction peak with increasing Higgs boson mass is the direct consequence of the existence of the additional hard scale  $M_H$ , which makes the interaction radius smaller. The  $\xi$  dependence is shown in Fig.4.

The second result is the total cross-section versus Higgs boson mass. We obtain the following results for the total cross-section of the EDD Higgs boson production:

$c_{gp}$	$M_H$ (GeV)	$\sigma_{p+p \rightarrow p+H+p}$ (fb)			
		LHC		TeVatron	
		no Sud. suppr.	Sud. suppr.	no Sud. suppr.	Sud. suppr.
3.5	100 $\rightarrow$ 500	110 $\rightarrow$ 57	4.6 $\rightarrow$ 0.14	12 $\rightarrow$ 0.4	0.5 $\rightarrow$ 0.001
2.3(3.3)	100 $\rightarrow$ 500	20 $\rightarrow$ 11	<b>3.6 <math>\rightarrow</math> 0.11</b>	2.2 $\rightarrow$ 0.08	0.4 $\rightarrow$ 0.0009

The above results for LHC energies are depicted in Figs.5-8. The form of the curve originates from the standard gluon-gluon-Higgs vertex and has a peak near  $M_H \simeq 2m_t$ . For the case of Sudakov-like suppression the cross-section vanishes faster with  $M_H$ .

It is useful to compare our result with other studies. Results quite close to ours (with the normalization to the CDF data,  $c_{gp} = 3.3$ ) were given in Ref. [8], where the value of the total cross-section is about 3 fb. In both cases the most important suppressing in the mass region  $M_H > 100$  GeV is due to (perturbative) Sudakov factors, while the nonperturbative (absorbitive) factors play relatively minor role.

Results of other authors were considered in details in [9]. The highest cross-section 2 pb for  $M_H = 400$  GeV at LHC energies was obtained in Ref. [10]. They used a nonfactorized form of the amplitude and a "QCD inspired" model for  $gp \rightarrow gp$  amplitudes, taking into account the nonperturbative proton wave functions. Even if we multiply the result of

Ref. [10] by the suppressing factor, it will be larger than ours. This could serve as the indication of the role of nonperturbative effects. Our model is based on the Regge-Eikonal approach for the amplitudes, which is primordially nonperturbative, normalized to the data from HERA on  $\gamma p \rightarrow J/\Psi p$  and improved by the CDF data on the exclusive di-jet production.

To estimate the signal to QCD background ratio for  $b\bar{b}$  signal we use the standart expression for  $gg \rightarrow b\bar{b}$  amplitude and assumptions [11]-[14]:

- possibility to separate final  $b\bar{b}$  quark jets from gluon jets. If we cannot do it, it will increase the background by two orders of magnitude under the 50% efficiency.
- suppression due to the absence of colour-octet  $b\bar{b}$  final states
- suppression of light fermion pare production, when  $J_{z,tot} = 0$  (see also [15],[16])
- cut  $E_T > 50$  GeV ( $\theta \geq 60^\circ$ ), since the cross-section of diffractive  $b\bar{b}$  jet production strongly decreases with  $E_T$ .

The theoretical result of these numerical estimations is

$$\begin{aligned} \frac{Signal(pp \rightarrow pHp \rightarrow pb\bar{b}p)}{QCD \ background} &\geq \\ &\geq 9.5 \cdot 10^{-6} |f|^2 Br_{H \rightarrow Q\bar{Q}} \frac{M_H^3}{\Delta M}, \end{aligned} \quad (22)$$

where  $|f|^2 \simeq 0.5 \rightarrow 3$  for Higgs boson masses  $100 \rightarrow 350$  GeV. For  $M_H \simeq 115$  GeV

$$\frac{Signal(pp \rightarrow pHp \rightarrow pb\bar{b}p)}{QCD \ background} \geq 3.8 \frac{GeV}{\Delta M}, \quad (23)$$

where  $\Delta M$  is the mass resolution of the detector. Similar result was strictly obtained in [11],[12]. More exact estimations of the above ratio by fast Monte-Carlo simulations and the total efficiency of EDD Higgs boson production will be publised in a forthcoming paper.

## 4 Conclusions

We see from the result that there is a real possibility to detect Higgs boson using the usual  $b\bar{b}$  signal under the luminosity greater than  $10^{32}$  in EDD events at LHC. Accuracy of the mass measurements could be improved by applying the missing mass method [17].

The low value of the exclusive Higgs boson production cross-section obtained in this paper is mainly due to the Sudakov suppression factor (18), the full validity of which is not obvious for us, because the confinement effects can strongly modify the "real gluon emission".

It is interesting that in spite of different models and quite different ways of account of absorbtive effects in our paper and in Ref. [8], the final results (see Fig.8) appeared to be quite close.

Certainly, the cross-sections may be several times larger due to still not very well known non-perturbative factors.

It is possible to generalize our approach for the exclusive production of other particles like  $\chi_{c0}$ ,  $\chi_{b0}$ , radion, K.-K. gravitons, glueballs. In this case cross-sections can be larger than for EDD Higgs boson production, and some other important investigations like partial wave analysis and measurements of the diffractive pattern of the interaction could be done.

## Acknowledgements

We are grateful to A. De Roeck, A. Prokudin, A. Rostovtsev, A. Sobol, S. Slabospitsky and participants of BLOIS2003 workshop and several CMS meetings for helpful discussions. This work is supported by the Russian Foundation for Basic Research, grant no. 02-02-16355

## References

- [1] V.A. Petrov, Proc. of the 2nd Int. Symp. "LHC: Physics and Detectors". (Eds. A.N. Sissakian and Y.A. Kultchitsky), June 2000, Dubna. P.223; V.A. Petrov, A.V. Prokudin, S.M. Troshin, N.E. Tyurin, *J. Phys. G: Nucl. Part. Phys.* **27** (2001) 2225.
- [2] V.A. Petrov, *Proceedings of the VIIth Blois Workshop* (Ed. M. Haguenauer et al., Editions Frontieres; Paris 1995).
- [3] V.A. Petrov and A.V. Prokudin, *Phys. Atom. Nucl.* **62** (1999) 1562.
- [4] A. Kniehl, *Phys. Rept.* **240** (1994) 211.
- [5] A. Berera, J. C. Collins, *Nucl. Phys. B* **474** (1996) 183.
- [6] V.A. Petrov, A. V. Prokudin, *Eur.Phys.J.C* **23** (2002)135.
- [7] CDF Collaboration (K. Borras for the collaboration). FERMILAB-CONF-00-141-E, Jun 2000; K. Goulianos, talk given in the Xth Blois workshop, 2003, Helsinki, Finland; M. Gallinaro, hep-ph/0311192.
- [8] V. A. Khoze, A. D. Martin and M. G. Ryskin, *Eur. Phys. J. C* **14** (2000) 525; *Eur. Phys. J. C* **21** (2001) 99; V. A. Khoze, hep-ph/0105224;
- [9] V. A. Khoze, A. D. Martin, M. G. Ryskin, *Eur. Phys. J. C* **26** (2002) 229.
- [10] J.-R. Cudell and O. F. Hernandez, *Nucl. Phys. B* **471** (1996) 471.
- [11] V. A. Khoze, A. D. Martin, M. G. Ryskin, *Eur. Phys. J. C* **19** (2001) 477.



- [12] A. De Roeck, V. A. Khoze, A. D. Martin, R. Orava, M. G. Ryskin, *Eur. Phys. J. C* 25 (2002) 391.
- [13] V. A. Khoze, A. D. Martin, M. G. Ryskin, *Eur. Phys. J. C* 23 (2002) 311.
- [14] A. D. Martin, M. G. Ryskin and V. A. Khoze, *Phys. Rev. D* 56 (1997) 5867.
- [15] A. Bialas and V. Szeremeta, *Phys. Lett. B* 296 (1992) 191;  
A. Bialas and R. Janik, *Z. Phys. C* 62 (1994) 487.
- [16] J. Pumplin, *Phys. Rev. D* 52 (1995) 1477.
- [17] M.G. Albrow and A. Rostovtsev, FERMILAB-PUB-00-173. Aug. 2000.

## Figure captions

Fig. 1: The full unitarization of the process  $p + p \rightarrow p + X + p$ .

Fig. 2: The process  $p + p \rightarrow p + H + p$ . Absorbtion in the initial and final pp-channels is not shown.

Fig. 3: t-distribution  $d\sigma/dt/\sigma_{tot}$  of the process  $p + p \rightarrow p + H + p$  for Higgs boson masses 100 and 500 GeV.

Fig. 4:  $\xi$ -distribution  $d\sigma/d\xi/\sigma_{tot}$  of the process  $p + p \rightarrow p + H + p$  for  $M_H = 100$  GeV.

Fig. 5: The total cross-section (in fb) of the process  $p + p \rightarrow p + H + p$  versus Higgs boson mass for  $c_{gp} = 3.5$  without Sudakov-like suppression.

Fig. 6: The total cross-section (in fb) of the process  $p + p \rightarrow p + H + p$  versus Higgs boson mass for  $c_{gp} = 3.5$  with Sudakov-like suppression.

Fig. 7: The total cross-section (in fb) of the process  $p + p \rightarrow p + H + p$  versus Higgs boson mass for  $c_{gp} = 2.3$  without Sudakov-like suppression.

Fig. 8: The total cross-section (in fb) of the process  $p + p \rightarrow p + H + p$  versus Higgs boson mass for  $c_{gp} = 3.3$  with Sudakov-like suppression.

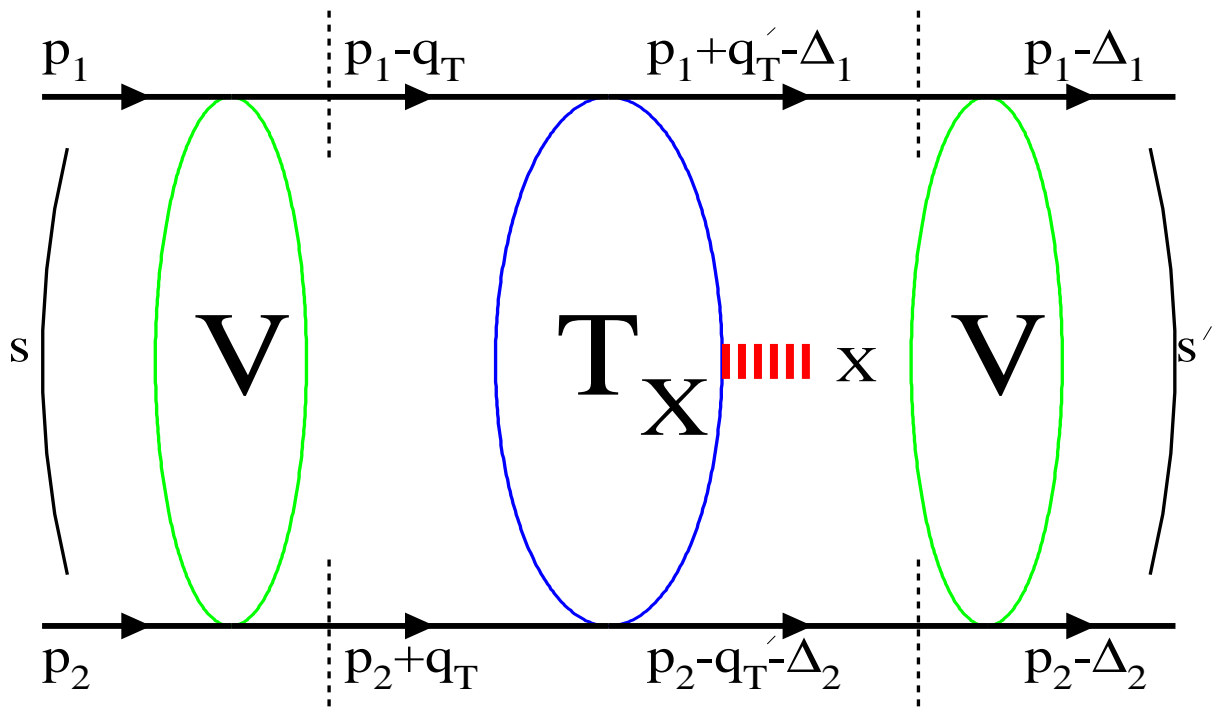


Figure 1:

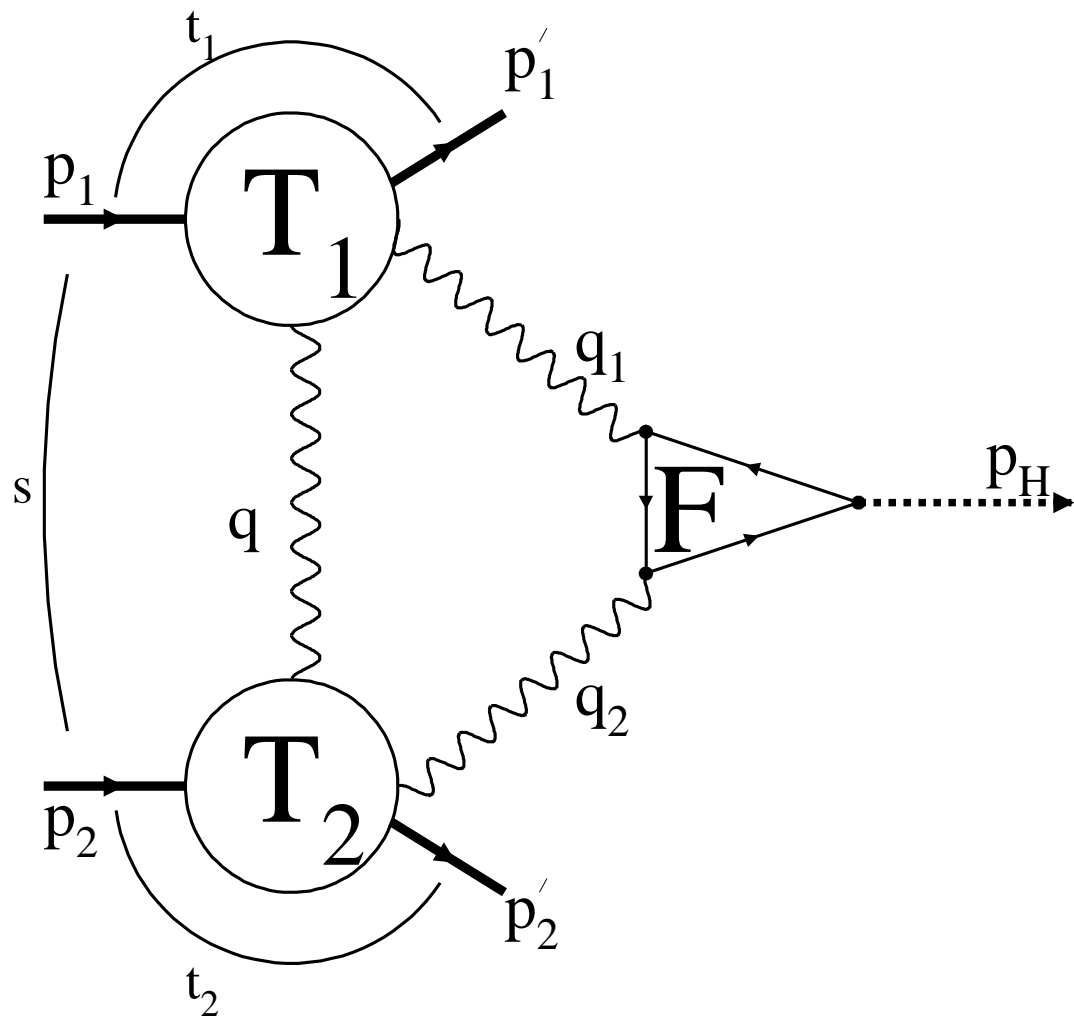


Figure 2:

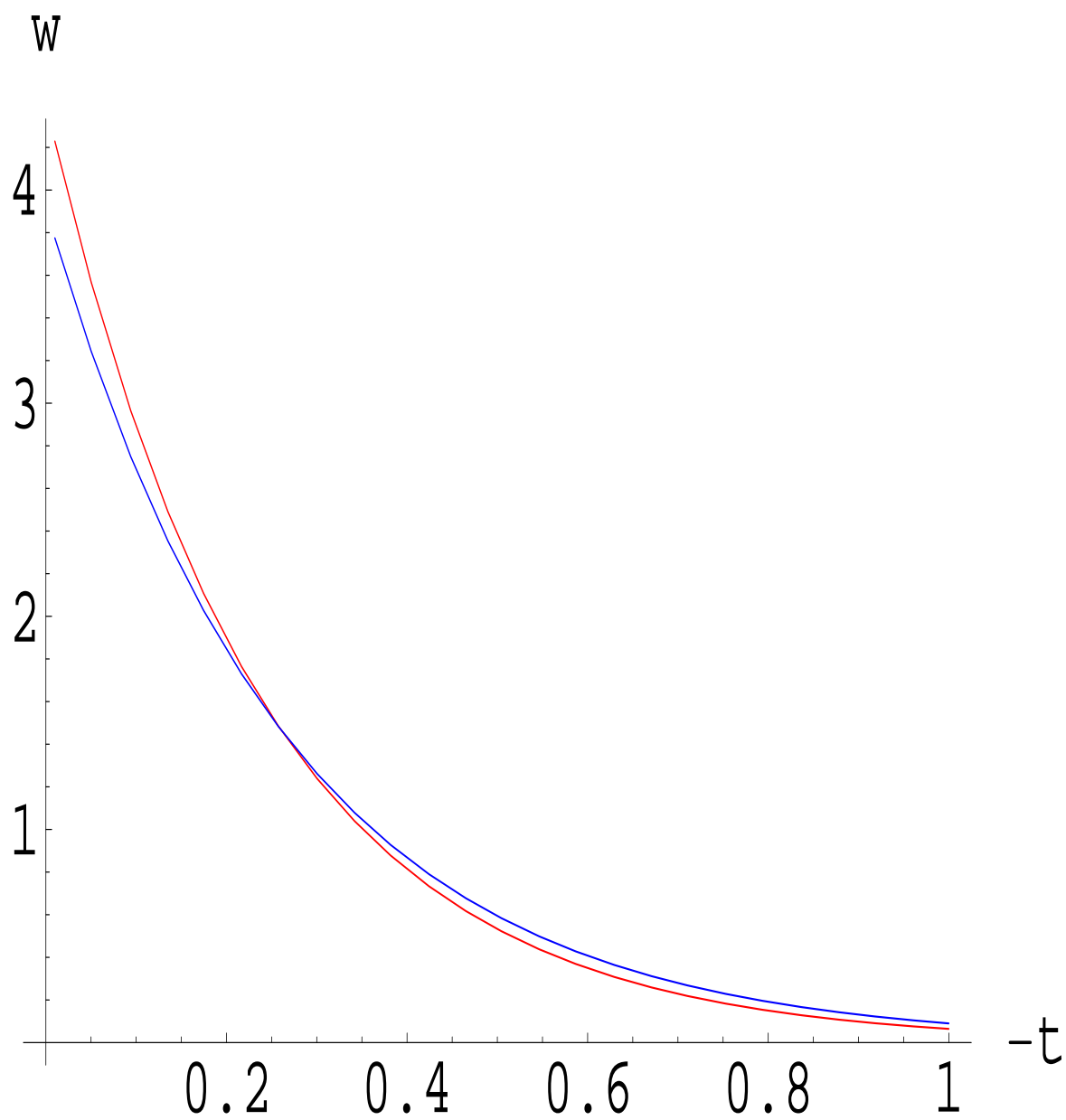


Figure 3:

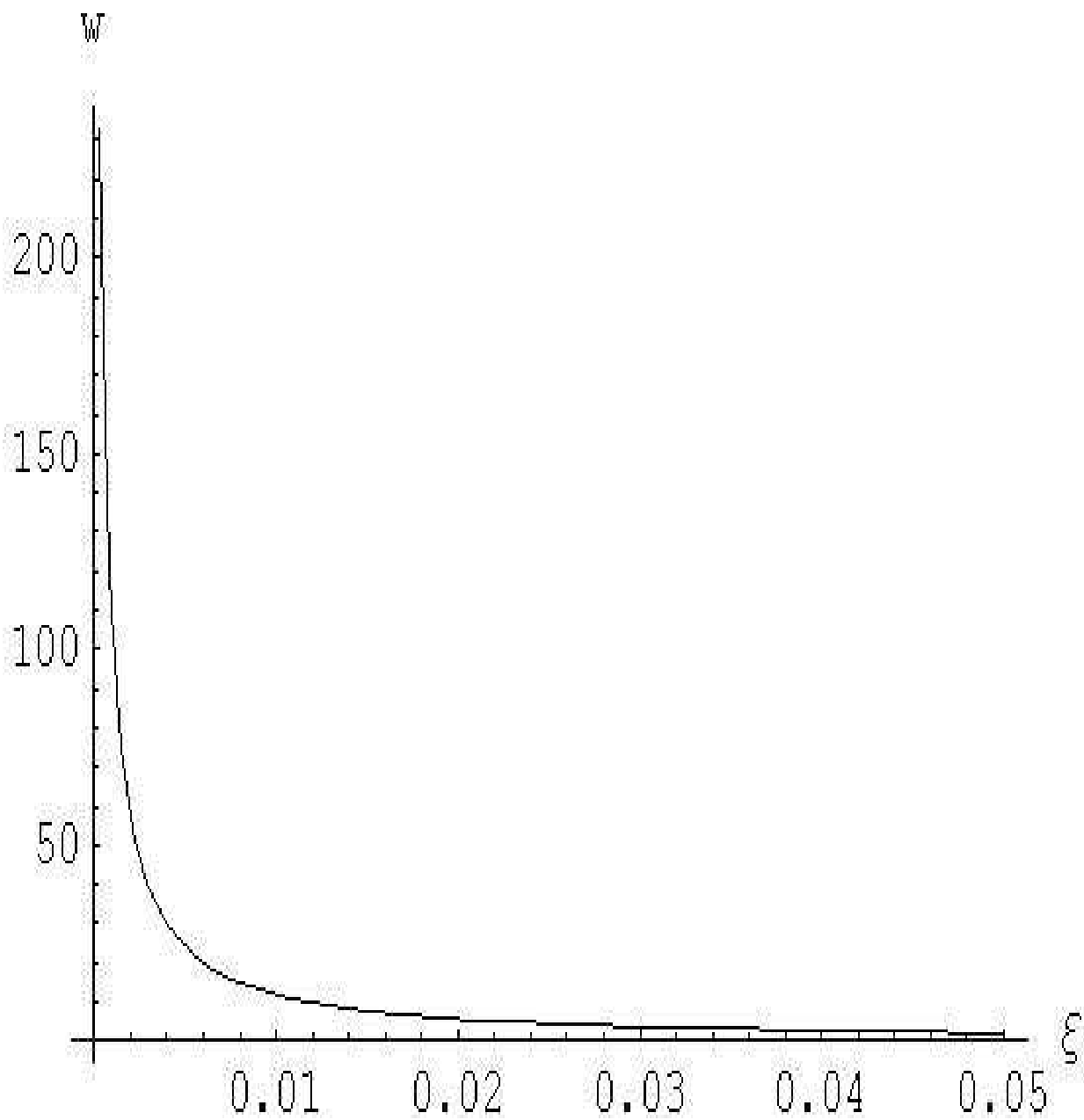


Figure 4:

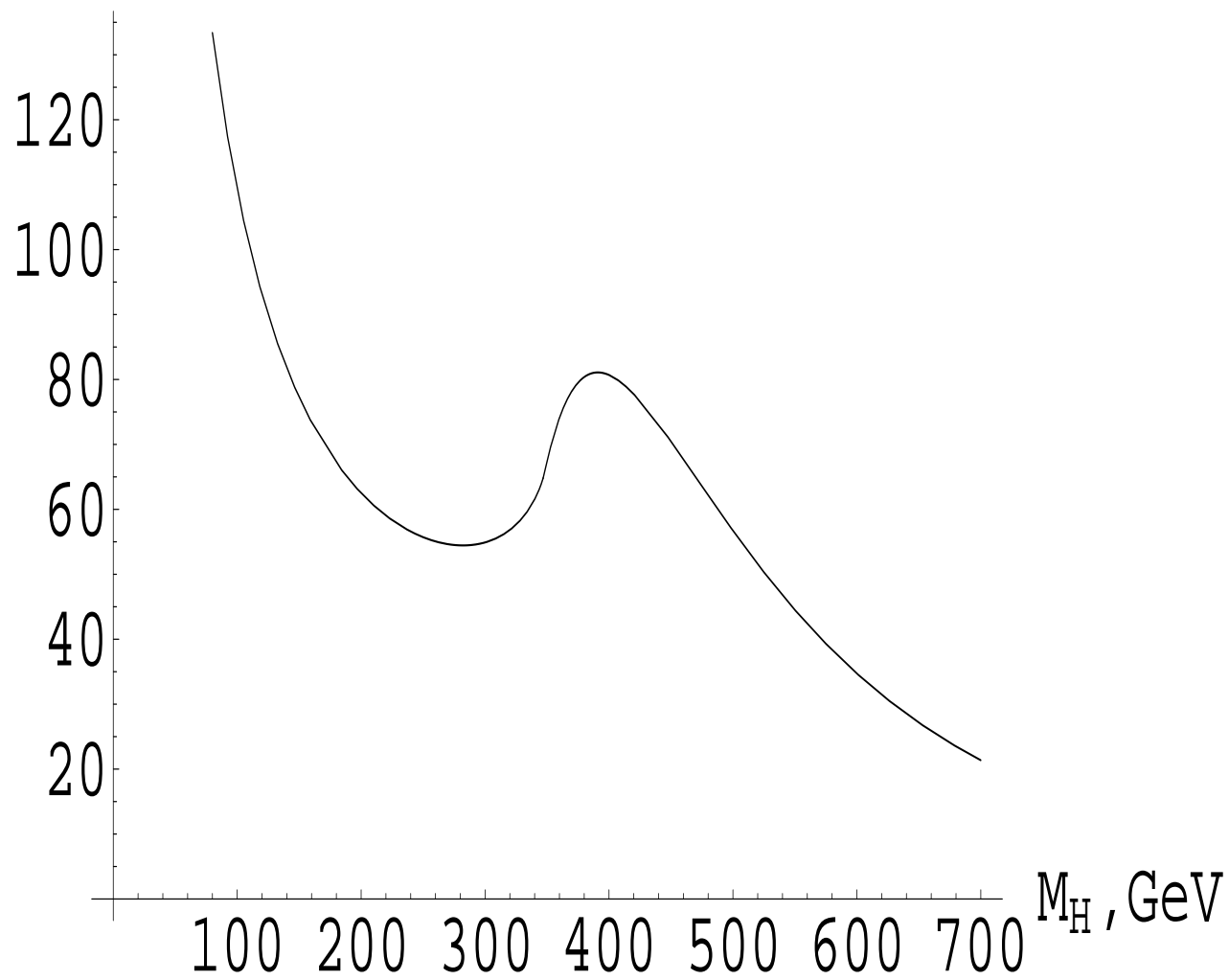


Figure 5:

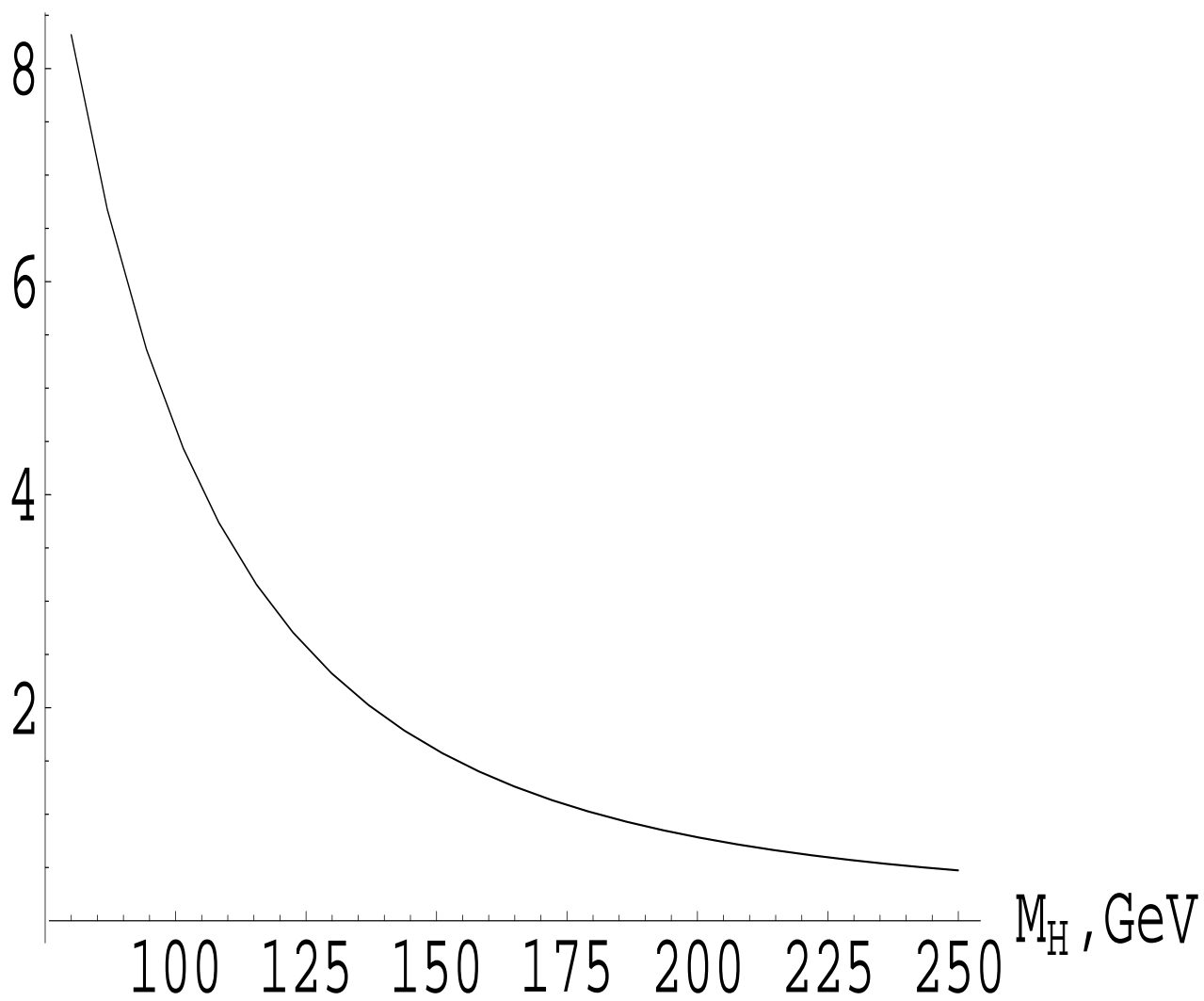


Figure 6:



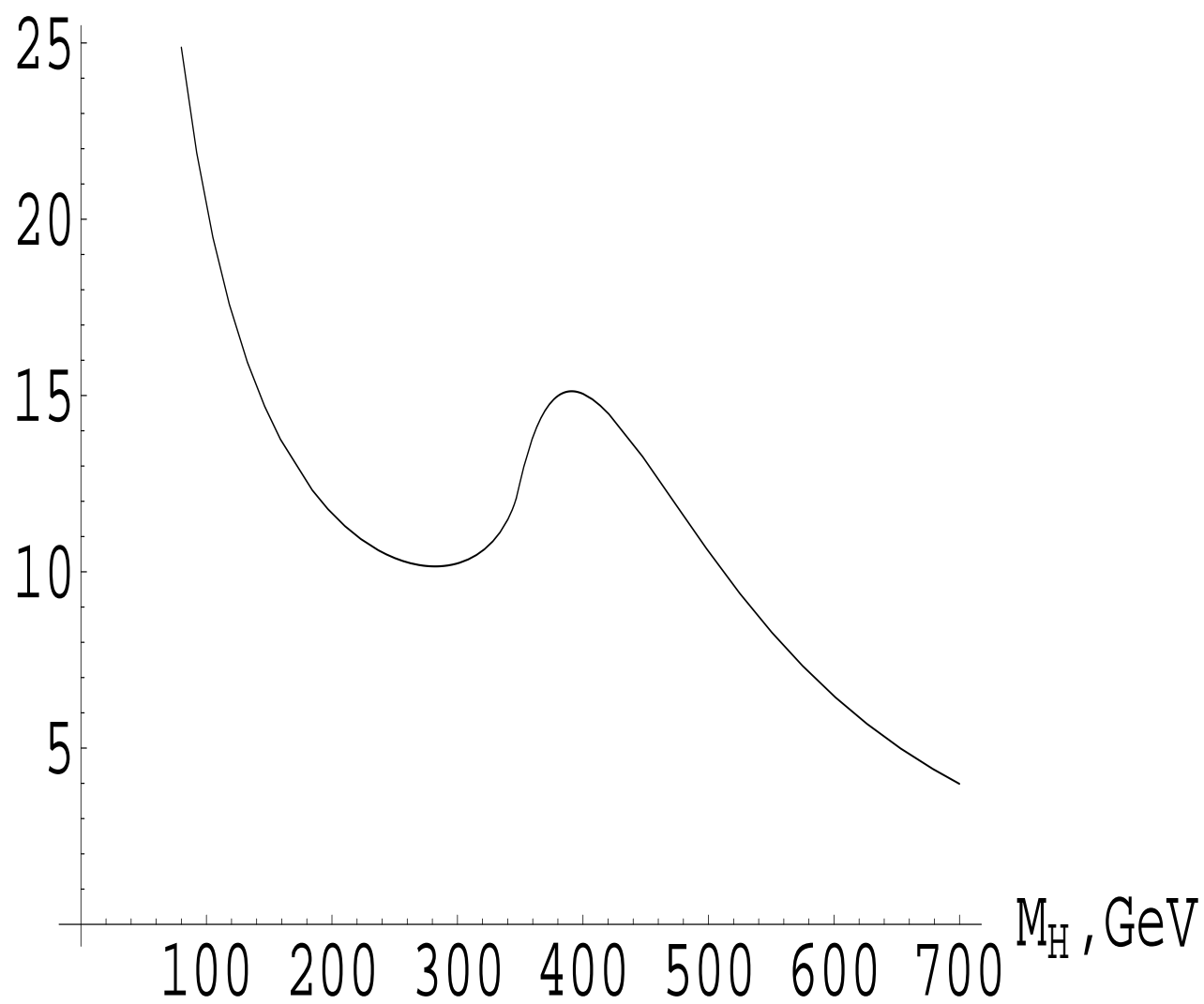


Figure 7:

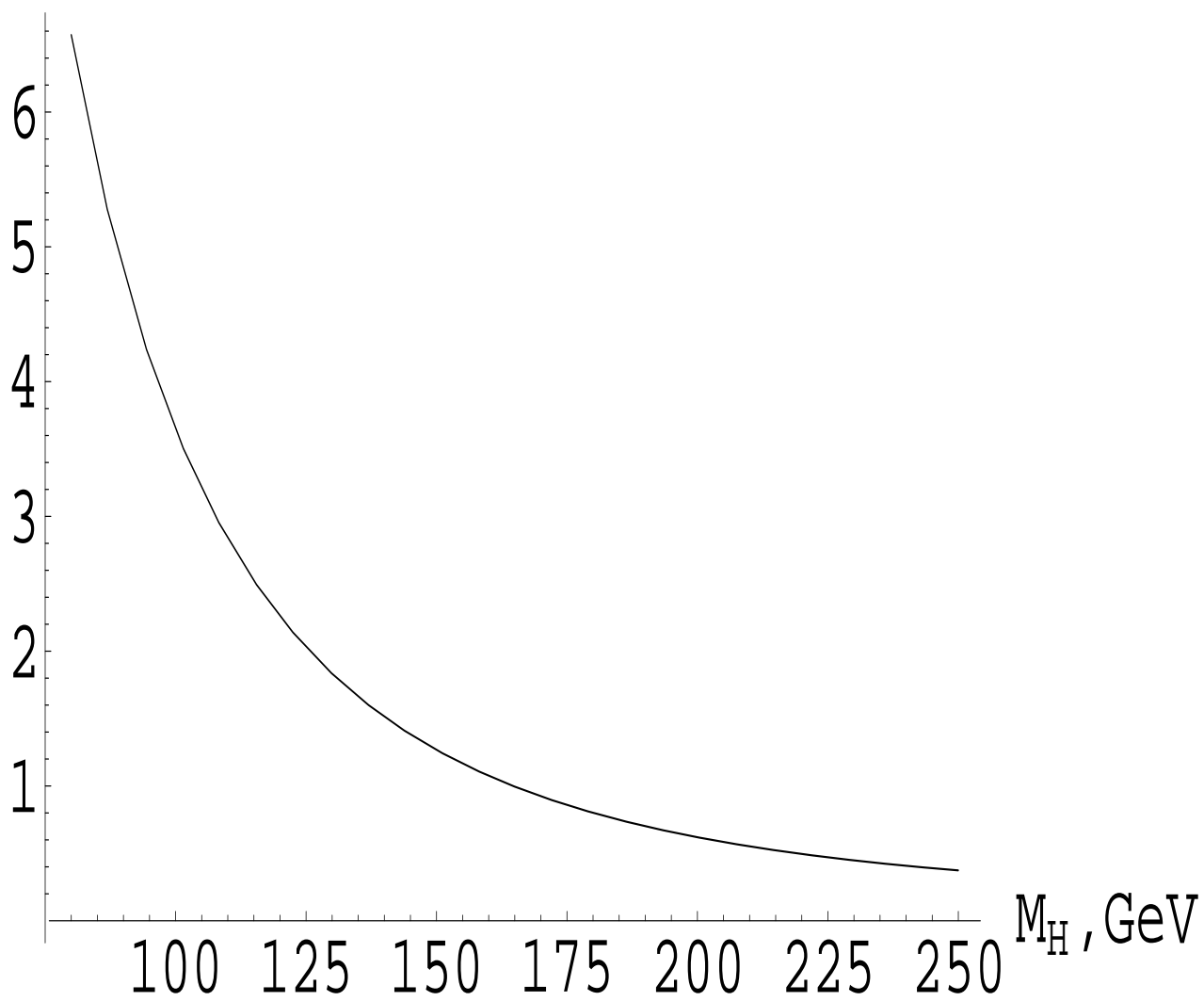


Figure 8: